Revealing Extremely Low Energy Amplitude Modes in the Charge-Density-Wave Compound $LaAgSb_2$

R. Y. Chen,[1,2] S. J. Zhang,[1] M. Y. Zhang,[1] T. Dong,[1] and N. L. Wang[1,3,*]
[1]International Center for Quantum Materials, School of Physics, Peking University, Beijing 100871, China
[2]Center for Advanced Quantum Studies, Department of Physics, Beijing Normal University, Beijing 100875, China
[3]Collaborative Innovation Center of Quantum Matter, Beijing 100871, China

(Received 29 October 2016; revised manuscript received 16 January 2017; published 7 March 2017)

Using infrared spectroscopy and ultrafast pump probe measurement, we have studied the two charge-density-wave (CDW) instabilities in the layered compound $LaAgSb_2$. The development of CDW energy gaps was clearly observed by optical spectroscopy, which removed most of the free carrier spectral weight. More interestingly, our time-resolved measurements revealed two coherent oscillations that softened by approaching the two phase transition temperatures, respectively. We addressed that these two oscillations come from the amplitude modes of CDW collective excitations, the surprisingly low energies (0.12 THz and 0.34 THz for the higher and lower temperature ones, respectively) of which are associated with the extremely small nesting wave vectors. Additionally, the amplitude and relaxation time of photoinduced reflectivity of $LaAgSb_2$ single crystals stayed unchanged across the CDW phase transitions, which is quite rare and deserves further investigation.

DOI: 10.1103/PhysRevLett.118.107402

The charge-density wave (CDW) is one of the most fundamental collective quantum phenomena in solids. Charge density waves display periodic modulations of the charge with a period which is commensurate or incommensurate with the underlying lattice. Most CDW states are driven by the nesting topology of Fermi surfaces (FSs), i.e., the matching of sections of FSs to others by a wave vector $\mathbf{q} = 2\mathbf{k}_F$, where the electronic susceptibility has a divergence. A single-particle energy gap opens in the nested regions of the FSs at the transition, which leads to the lowering of the electronic energies of the system. Simultaneously, the phonon mode of the acoustic branch becomes softened to zero frequency at $\mathbf{q} = 2\mathbf{k}_F$ as a result of electron-phonon interaction, which further leads to the periodic modulation of the lattice structure.

CDW also has collective excitations referred to as amplitude mode (AM) and phase mode. Phase excitation corresponds to the translational motion of the undistorted condensate. In the $\mathbf{q} = 0$ limit, the phase mode should locate at zero energy in an ideal case since the translational motion does not change the condensation energy [1]. In reality, due to the presence of impurities or defects, the phase mode is pinned at a finite frequency, usually in the microwave frequency range. The pinning or depinning of phase mode has a dramatic effect on charge transport properties [2–4]. On the other hand, the amplitude mode involves the ionic displacement and has a finite energy even at the $\mathbf{q} = 0$ limit. For most CDW materials, the amplitude mode has an energy scale of about 10 meV (or ~2 THz) [5–11]. Because of the presence of such a gap for the amplitude mode (i.e., the mode energy at $\mathbf{q} = 0$), its effect on low temperature physical properties of CDW condensate has been much less studied. Generally, amplitude modes can be treated as optical phonons, reflecting the oscillations of ions. Nevertheless, it is also proposed to be intimately related to the modulation of the CDW energy gap [12,13], which is the most fundamental difference between AM and optical phonons.

The compound $LaAgSb_2$, which crystallizes in simple tetragonal $ZrCuSi_2$ structures as shown in the lower inset of Fig. 1(a), was revealed to experience two CDW phase transitions around $T_{C1} = 207$ K and $T_{C2} = 184$ K [14], providing a unique platform to study the effect of amplitude modes on physical properties, as will be elaborated below. The electronic band structure calculation reveals that there are four bands crossing the Fermi energy E_F, consistent with de Haas–van Alphen (dHvA) measurement [15], and the two CDW modulations are dominantly driven by the FS nesting [16]. Recently, some renewed interest has been triggered in the $LaAgSb_2$ compound because of the possibility of hosting Dirac fermions in this material. First-principles calculation demonstrated that there are both linear and parabolic bands crossing the Fermi level, which was supported by the appearance of large linear magnetoresistance [17]. In addition, angle-resolved photoemission spectroscopy (ARPES) directly observed the Dirac-conelike structure in the vicinity of the Fermi level, which was formed by the crossing of two linear Sb $5p_{x,y}$ energy bands [18]. Of most significance, the nested FS associated with CDW phase transition was proved to emerge from two almost parallel segments of the Dirac cone, leading to a very small modulation wave vector $2\mathbf{k}_F$.

To investigate the potential relationship between Dirac fermions and CDW orderings and to gain insight into the possible effect of AM, we performed infrared spectroscopy

and an ultrafast pump probe measurement—both of which are supposed to be very sensitive to the formation of symmetry breaking gaps—on the single crystalline $LaAgSb_2$. Particularly, the ultrafast spectroscopy is playing a more important role than ever in studying the coherent vibrational dynamics since this method can easily access oscillations of an extremely low energy scale as an extension of neutron and Raman scattering.

We have successfully synthesized large pieces of $LaAgSb_2$ single crystals by the self flux method [14]. The platelike samples have shiny surfaces after eliminating the extra flux by a centrifugal machine. The in-plane reflectivity $R(\omega)$ was measured by the combination of Fourier transform infrared spectrometer Bruker 113 V and 80 V in the frequency range from 30 to 25000 cm^{-1}.

As displayed in the upper inset of Fig. 1(a), the room temperature reflectivity was characterized by typical metallic responses: $R(\omega)$ approaches the unit at zero frequency, and a well-defined plasma edge was clearly observed around 10000 cm^{-1}. The reflectivity spectrum of 200 K almost overlaps with that of 220 K in the normal state. Although the first CDW instability has already set in at

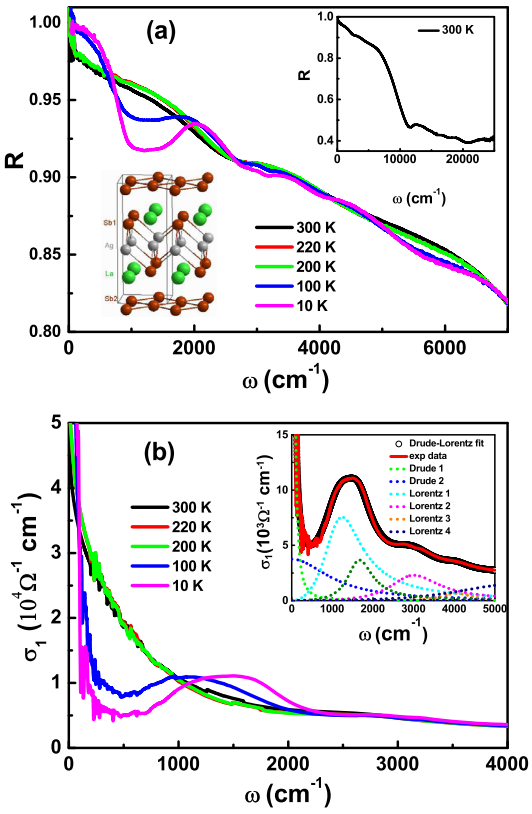

FIG. 1. The temperature-dependent (a) reflectivity $R(\omega)$ and (b) optical conductivity $\sigma_1(\omega)$ for the $LaAgSb_2$ single crystal below 7000 cm^{-1} and 4000 cm^{-1}, respectively. The insets of (a) present crystal structure and $R(\omega)$ at 300 K over a broad frequency range up to 25000 cm^{-1}. The inset of (b) displays $\sigma_1(\omega)$ at 10 K together with a Drude-Lorentz fit.

200 K, the modification of the electronic band structure is yet too weak to be detected. With temperature further cooling far below T_{C2}, a pronounced dip structure appears roughly between 1000–2000 cm^{-1}, which strongly evidences the formation of a charge gap in the vicinity of the Fermi level due to the development of the CDW order.

The real part of optical conductivity $\sigma_1(\omega)$ was derived from $R(\omega)$ through Kramers-Kronig transformation [19], as shown in Fig. 1(b). In the normal state, the optical conductivity exhibits clear Drude peaks centered at zero frequency, and the broad half width indicates a large scattering rate γ of the free carriers. Upon entering the CDW state, the spectral weight of the Drude peak was substantially removed and transferred to higher energies, and a broad bump locating around 1000 cm^{-1} emerges. Moreover, the bump position shifted to higher energies as the temperature decreases. In fact, these features are the spectroscopic fingerprints of density wave materials since the case-I coherence factor of density wave order is expected to cause a sharp rise in the optical conductivity spectrum just above the energy gap [1]. Here, we can roughly take the central position of the emerging bump as the energy scale of the CDW gap.

To make the estimation more accurate, we have employed the Drude-Lorentz model to fit the optical conductivity,

$$\epsilon(\omega) = \epsilon_\infty - \sum_s \frac{\omega_{ps}^2}{\omega^2 + i\omega/\tau_{Ds}} + \sum_j \frac{S_j^2}{\omega_j^2 - \omega^2 - i\omega/\tau_j}.$$

Here, ε_∞ stands for the dielectric constant at high energy; the middle and last terms are the Drude and Lorentz components, respectively. We found that the $\sigma_1(\omega)$ can be well reproduced by two Drude terms and several Lorentz terms. The bump appearing at a low temperature is too broad to be reproduced by a single Lorentz term, demonstrating possibly two different gap openings associated with the CDW phase transitions. According to our experimental configuration, the obtained $\sigma_1(\omega)$ is supposed to be parallel with the ab plane; thus, the observed charge gaps shall be originated from the CDW order with higher transition temperature. The obtained gap energies are about 1240 cm^{-1} (~154meV) and 1670cm^{-1} (~207meV), respectively. The number of lost free carriers could be estimated by the variation of plasma frequency $\omega_p \sim \sqrt{n/m^*}$, where n and m^* represent the number and effective mass of free carriers, respectively. As we have employed two Drude terms to fit $\sigma_1(\omega)$, the overall plasma frequency was obtained by $\omega_p = (\omega_{p1}^2 + \omega_{p2}^2)^{1/2}$, where ω_{p1} and ω_{p2} represent the individual plasma frequencies corresponding to the respective Drude component. According to our fitting procedure, as presented in the inset of Fig. 1(b), ω_p varies from 40400 cm^{-1} at room temperature to 25500 cm^{-1} at 10 K, which indicates that about 60% of free carriers are removed by the opening of CDW gaps. Meanwhile, the scattering rate γ_1 decreases violently from 457 cm^{-1} to

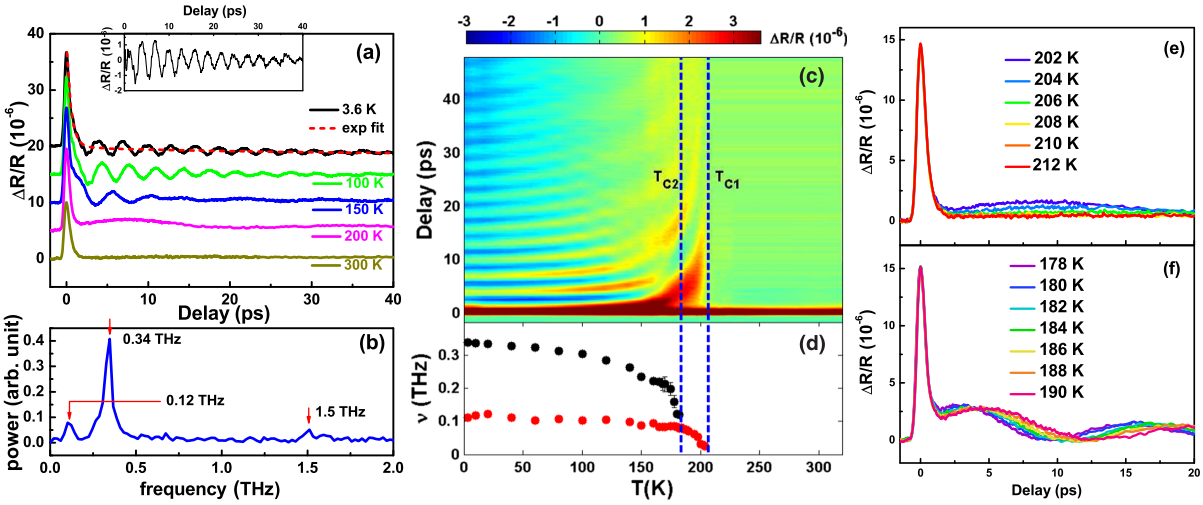

FIG. 2. (a) The photoinduced reflectivity $\Delta R/R$ as a function of time delay at several selected temperatures. The experimental data are shifted upwards for the sake of clearness. The red dotted line is the exponential fitting of $\Delta R/R$ at 3.6 K. The inset shows the oscillation part of $\Delta R/R$ as described in the main text. (b) The fast Fourier transformation of the oscillation part of $\Delta R/R$ at 3.6 K. (c) The photoinduced reflectivity $\Delta R/R$ as a function of time delay and temperature. (d) The temperature-dependent frequencies of the two CDW amplitude modes ν_1 (red dot) and ν_2 (black dot). (e) The photoinduced reflectivity $\Delta R/R$ across the first CDW phase transition and (f) the second CDW phase transition.

14 cm^{-1}, and γ_2 also reduces from 2073 cm^{-1} to 1097 cm^{-1}, evidenced by the narrowing of Drude peaks, which makes the compound an even better metal in spite of the substantial carrier density loss.

Some more interesting properties of this material have been revealed by our ultrafast pump probe measurement, which has been proven to be particularly powerful in detecting both the single-particle excitations across small energy gaps [20–23] and the collective excitations relevant to quantum orderings [8,24,25]. We used a Ti:sapphire oscillator as the light source for both pump and probe beams, which can produce an 800 nm pulsed laser at 80 MHz repetition. The 100 femtosecond time duration of the laser pulses enables ultrashort time-resolved measurement. The fluence of the pump beam is about 2 $\mu J/cm^2$, and the fluence of the probe beam is ten times lower.

The photoinduced transient reflectivity $\Delta R/R$ at several selected temperatures are displayed in the main panel of Fig. 2(a) as a function of time delay. At room temperatures, $\Delta R/R$ initially increases in a very short time due to the pump excitation, then drops rapidly back to the equilibrium state within picoseconds, the falling slope of which could be well described by a single exponential decay, $\Delta R/R = A\exp(-t/\tau)$, where A represents the amplitude of the photoinduced reflectivity and τ stands for the relaxation time of the decay. Remarkably, pronounced oscillatory signals were observed at lower temperatures, the periodic time of which changes dramatically with temperature variation. In order to analyze the oscillatory component quantitatively, we first subtracted the exponential fitting part, as shown in Fig. 2(a) by the red dotted line for $T = 3.6$ K. The fast Fourier transformation of the residual part, as shown in the inset of this figure, demonstrated the frequencies of the oscillations. It is clearly seen in Fig. 2(b) that there are three distinct modes at 3.6 K, the frequencies of which are about 0.12 THz, 0.34 THz, and 1.5 THz, respectively. It should be noted that the 0.12 THz oscillation is out of the resolution limit of neutron and Raman scattering.

In order to investigate the origination of these oscillations, we have explored their temperature dependence thoroughly from 3.6 K to 320 K. The raw experimental data for all the measured temperature ranges were plotted in a pseudocolor picture, as shown in Fig. 2(c). The oscillatory components, which show up abruptly just below T_{C1}, were highlighted by setting the colorbar in a small amplitude scale. The frequencies' evolution of the oscillations as a function of temperature were displayed in Fig. 2(d), yielded by fast Fourier transformation. The one located around 1.5 THz is only visible at very low temperatures, and its frequency did not change with temperature, probably associated with a coherent phonon, so we did not show it in this figure. The mode $\nu_1 = 0.12$ THz is almost temperature independent at low temperature, but exhibits dramatic softening on approaching T_{C1}. It proceeds in a fashion very similar with the BCS gap function, indicating that ν_1 is probably the amplitude mode of the first CDW ordering. Analogously, $\nu_2 = 0.34$ THz softens significantly around T_{C2}, implying the appearance of another amplitude mode.

We have also carried out a fluence-dependent measurement at 10 K, as displayed in Fig. 3(a). It is found that if scaling $\Delta R/R$ by pump fluence, shown in the inset of Fig. 3(a), then the renormalized transient reflectivities almost overlap with each other, indicating that the

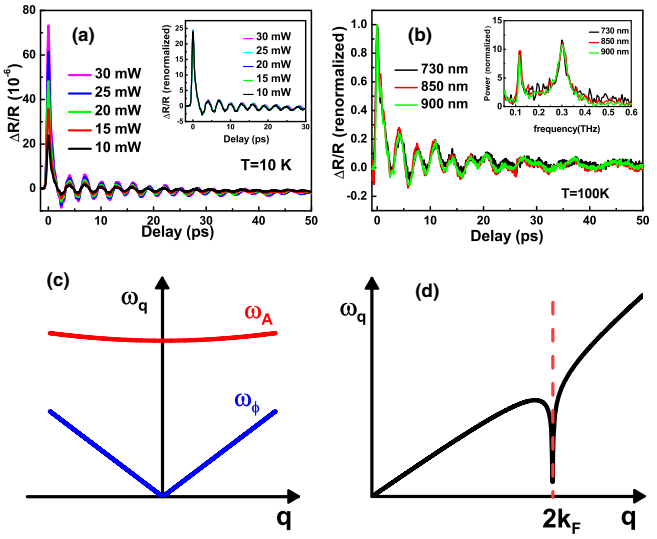

FIG. 3. (a) The photoinduced reflectivity under different pump power. The illuminating spot remains unchanged during the measurement, and 10 mW give rise to a fluence of about 2 $\mu J/cm^2$. The inset shows renormalized $\Delta R/R$ scaled by the pump power. (b) The renormalized photoinduced reflectivity obtained by different pump and probe wavelengths at 100 K. The inset displays the fast Fourier transformation of the oscillation part corresponding to different wavelengths. (c) Amplitude and phase mode dispersion relations. (d) Softening of acoustic phonon mode at CDW wave vector $2\mathbf{k}_F$.

frequencies of ν_1 and ν_2 are basically independent of pump fluence. The good overlapping also suggested that the amplitude of both the single exponential part and the oscillating part increase linearly with pump fluence increasing, which is in accordance with amplitude mode behavior. Subtle deviation from perfect overlap in the long time term is due to the heating effect of laser illumination. Nevertheless, such oscillation observed in the time domain could also be connected to coherence lattice vibrations, such as nonequilibrium phonon dynamics, which may emerge upon entering the CDW state due to lattice distortion accompanied by the phase transition [26]. Furthermore, the surprisingly low energy scales of both ν_1 and ν_2 are rarely seen for amplitude mode of CDW orderings, whose magnitude is usually one or a few terahertz. On the contrary, the frequencies of the acoustic phonon and phase mode of the CDW ordering locate generally in the sub-THz area [27,28], consistent with our experimental results.

To exclude the possibility of coherent acoustic phonon and phason, we further performed a wavelength-dependent measurement at a fixed temperature of 100 K. The wavelengths of both pump and probe pulses were tuned to 730 nm, 850 nm, and 900 nm separately, and the obtained photoinduced signals are shown in the main panel of Fig. 3(b). There are actually no detectable differences between those signals corresponding to different wavelengths. In addition, the obtained frequencies were displayed in the inset of Fig. 3(b), all of which indicate two modes locating around 0.12 THz and 0.3 THz. It is well known that the frequency of amplitude mode exhibits a gap when the wave vector approaches zero, whereas the phase mode is gapless, as shown in Fig. 3(c). The dispersion of acoustic phonon is similar to that of phase mode. That is, the frequency of acoustic phonon shall increase with the probe wavelength decreasing [28]. Consequently, the contribution from acousticlike phonons, including phason for the modes observed in our experiments, could be ruled out immediately. It is also noted that the temperature dependence of optical phonons behaves quite differently from our results [29].

Now, we are quite certain that ν_1 and ν_2 come from the amplitude mode of the two CDW orderings. Remarkably, the frequencies of ν_1 and ν_2 are extraordinarily low. It is well known that the acoustic phonon softens significantly at $\mathbf{q} = 2\mathbf{k}_F$ upon the CDW phase transition, as exhibited in Fig. 3(d). Theoretical calculation suggested that the frequency of amplitude mode ω_A satisfies [1]

$$\omega_A = \left(\lambda\omega_{2k_F}^2 + \frac{1}{3}\frac{m}{m^*}V_F^2 q^2\right)^{1/2}, \quad (1)$$

where ω_{2k_F} is the frequency of the softening phonon above the phase transition temperature; λ and V_F are the electron-phonon coupling constant and Fermi velocity, respectively. In the $q = 0$ limit, $\omega_A \sim \lambda^{1/2}\omega_{2k_F}$. The modulation wave vectors of the two CDW orders in $LaAgSb_2$ were identified to be $\sim(0.026\,0\,0)$ for the higher temperature transition and $(0\,0\,0.16)$ for the lower one [16], both of which are uncommonly small, suggesting extremely long lattice modulation periods in the real space. As the softened phonon dispersion is of the acoustic type, the tiny modulation wave vectors directly lead to a low energy ω_{2k_F}, which further gives rise to rarely low energy amplitude modes ν_1 and ν_2. It is worth pointing out that the frequency of ν_1 is lower than ν_2, which is in good agreement with our interpretation because the modulation wave vector of the first phase transition is much smaller than the second one. Furthermore, our result also provided insight into the velocities V_{F1} and V_{F2} of corresponding acoustic phonon branches. The ratio between them is given by

$$\frac{V_{F1}}{V_{F2}} = \frac{\omega_{2k_{F1}}/2k_{F1}}{\omega_{2k_{F2}}/2k_{F2}} \sim \frac{\nu_1/k_{F1}}{\nu_2/k_{F2}} \sim 2.2. \quad (2)$$

As mentioned above, the ultrafast pump probe measurement is very powerful in detecting the low energy gaps opening on the FS, such as density wave or superconducting gaps, which can be well explained by the phenomenological Rothwarth-Taylor (RT) model [30]. The two most pronounced features of relevant phase transitions are the significant enhancement of the amplitude A and the quasidivergence behavior of the relaxation time τ [20–23]. However, we did not observe either of such characters in $LaAgSb_2$ single crystals. As plotted in Figs. 2(e) and 2(f),

the single exponential part of $\Delta R/R$ remains unchanged across both of the two phase transitions, generating constant amplitude A and relaxation time τ. It seems that the CDW phase transitions do not have any effect on the transient reflectivity. To our knowledge, such an exotic phenomenon has never been observed ever before, and it is hard to understand, considering that more than half of the FSs are gapped by the CDW orders. Compared with other CDW materials, we highly suspect that the extraordinarily low energy AM may play some role in this case. Based on previous time-resolved ARPES measurement, the AM of CDW orders could induce periodic modulation of the conduction band, which further leads to CDW gap modulation [12,13]. Around the phase transition temperatures where the energy scales of gaps are actually very small, such modulation may probably melt the CDW gap within the time scale of the AM period, which is exceptionally long for $LaAgSb_2$. Consequently, the photoinduced $\Delta R/R$ does not change across the CDW phase transitions since the relaxation time is only about 0.5 ps.

In summary, we have utilized infrared and ultrafast pump probe spectroscopy to investigate the charge and coherent dynamics of the $LaAgSb_2$ single crystal. The optical conductivity revealed two energy gaps related to the higher temperature CDW phase transition, whose energy scales were identified to be 154 meV and 207 meV, respectively. More significantly, our time-resolved ultrafast measurement revealed two collective amplitude mode oscillations at surprisingly low energy scales of about 0.12 THz and 0.34 THz at the lowest temperature. This low energy scale implies that acoustic phonon mode, which softens and triggers CDW instability, also has a very low energy scale. We elaborate that those unusual properties are closely linked to the extremely small nesting wave vectors of the two CDW orders, which possibly results in the bizarre transient dynamics of the compound.

This work was supported by the National Science Foundation of China (No. 11327806 and No. GZ 1123), and the National Key Research and Development Program of China (No. 2016YFA0300902, and No. 2016YFA0302300). We acknowledge helpful discussions with Y. D. Quan and Z. P. Yin.

*nlwang@pku.edu.cn

[1] G. Grüner, *Density Waves in Solids* (Perseus, Cambridge, MA, 1994).
[2] A. Maeda, T. Furuyama, and S. Tanaka, Solid State Commun. **55**, 951 (1985).
[3] T. L. Adelman, S. V. Zaitsev-Zotov, and R. E. Thorne, Phys. Rev. Lett. **74**, 5264 (1995).
[4] R. M. Fleming and C. C. Grimes, Phys. Rev. Lett. **42**, 1423 (1979).
[5] J. C. Tsang, J. E. Smith, J. Watson, and M. W. Shafer, Phys. Rev. Lett. **37**, 1407 (1976).
[6] J. Demsar, K. Biljaković, and D. Mihailovic, Phys. Rev. Lett. **83**, 800 (1999).
[7] J. Demsar, L. Forró, H. Berger, and D. Mihailovic, Phys. Rev. B **66**, 041101 (2002).
[8] R. V. Yusupov, T. Mertelj, J.-H. Chu, I. R. Fisher, and D. Mihailovic, Phys. Rev. Lett. **101**, 246402 (2008).
[9] M. Lavagnini, M. Baldini, A. Sacchetti, D. Di Castro, B. Delley, R. Monnier, J.-H. Chu, N. Ru, I. R. Fisher, P. Postorino, and L. Degiorgi, Phys. Rev. B **78**, 201101 (2008).
[10] M. Porer, J. M. Ménard, H. Dachraoui, U. Leierseder, K. Groh, J. Demsar, U. Heinzmann, and R. Huber, *CLEO EUROPE/IQEC* (IEEE, Munich, Germany, 2013). p 1.
[11] T. Onozaki, Y. Toda, S. Tanda, and R. Morita, Jpn. J. Appl. Phys. **46**, 870 (2007).
[12] F. Schmitt, P. S. Kirchmann, U. Bovensiepen, R. G. Moore, L. Rettig, M. Krenz, J.-H. Chu, N. Ru, L. Perfetti, D. H. Lu, M. Wolf, I. R. Fisher, and Z.-X. Shen, Science **321**, 1649 (2008).
[13] H. Y. Liu, I. Gierz, J. C. Petersen, S. Kaiser, A. Simoncig, A. L. Cavalieri, C. Cacho, I. C. E. Turcu, E. Springate, F. Frassetto, L. Poletto, S. S. Dhesi, Z.-a. Xu, T. Cuk, R. Merlin, and A. Cavalleri, Phys. Rev. B **88**, 045104 (2013).
[14] K. Myers, S. Bud'ko, and I. Fisher, J. Magn. Magn. Mater. **205**, 27 (1999).
[15] K. D. Myers, S. L. Bud'ko, V. P. Antropov, B. N. Harmon, P. C. Canfield, and A. H. Lacerda, Phys. Rev. B **60**, 13371 (1999).
[16] C. Song, J. Park, J. Koo, K.-B. Lee, J. Y. Rhee, S. L. Bud'ko, P. C. Canfield, B. N. Harmon, and A. I Goldman, Phys. Rev. B **68**, 035113 (2003).
[17] K. Wang and C. Petrovic, Phys. Rev. B **86**, 155213 (2012).
[18] X. Shi, P. Richard, K. Wang, M. Liu, C. E. Matt, N. Xu, R. S. Dhaka, Z. Ristic, T. Qian, Y. F. Yang, C. Petrovic, M. Shi, and H. Ding, Phys. Rev. B **93**, 081105 (2016).
[19] D. B. Tanner, Phys. Rev. B **91**, 035123 (2015).
[20] J. Demsar, B. Podobnik, V. V. Kabanov, T. Wolf, and D. Mihailovic, Phys. Rev. Lett. **82**, 4918 (1999).
[21] E. E. M. Chia, D. Talbayev, J. X. Zhu, J. D. Thompson, A. J. Taylor, H. Q. Yuan, T. Park, C. Panagopoulos, G. F. Chen, J. L. Luo, and N. L. Wang, Phys. Rev. Lett. **104**, 027003 (2010).
[22] E. E. M. Chia, J.-X. Zhu, D. Talbayev, H. J. Lee, N. Hur, N. O. Moreno, R. D. Averitt, J. L. Sarrao, and A. J. Taylor, Phys. Rev. B **84**, 174412 (2011).
[23] R. Y. Chen, B. F. Hu, T. Dong, and N. L. Wang, Phys. Rev. B **89**, 075114 (2014).
[24] W. Albrecht, T. Kruse, and H. Kurz, Phys. Rev. Lett. **69**, 1451 (1992).
[25] J. Qi, T. Durakiewicz, S. A. Trugman, J.-X. Zhu, P. S. Riseborough, R. Baumbach, E. D. Bauer, K. Gofryk, J.-Q. Meng, J. J. Joyce, A. J. Taylor, and R. P. Prasankumar, Phys. Rev. Lett. **111**, 057402 (2013).
[26] H. Schäfer, V. V. Kabanov, M. Beyer, K. Biljakovic, and J. Demsar, Phys. Rev. Lett. **105**, 066402 (2010).
[27] D. Lim, V. K. Thorsmølle, R. D. Averitt, Q. X. Jia, K. H. Ahn, M. J. Graf, S. A. Trugman, and A. J. Taylor, Phys. Rev. B **71**, 1 (2005).
[28] Y. Ren, Z. Xu, and G. Lüpke, J. Chem. Phys. **120**, 4755 (2004).
[29] B. He, C. Zhang, W. Zhu, Y. Li, S. Liu, X. Zhu, X. Wu, X. Wang, H.-h. Wen, and M. Xiao, Sci. Rep. **6**, 30487 (2016).
[30] A. Rothwarf and B. N. Taylor, Phys. Rev. Lett. **19**, 27 (1967).